Multiple generations of grain aggregation in different environments preceded solar system body formation

Authors: H. A. Ishii[1]*, J. P. Bradley[1], H. A. Bechtel[2], D. E. Brownlee[3], K. C. Bustillo[4], J. Ciston[4], J. N. Cuzzi[5], C. Floss[6] and D. J. Joswiak[3]

Affiliations:

[1]Hawai‘i Institute of Geophysics and Planetology, University of Hawai‘i at Manoa, Honolulu, HI 96822, USA.

[2]Advanced Light Source Division, Lawrence Berkeley National Laboratory, Berkeley, CA 94720, USA.

[3]Department of Astronomy, University of Washington, Seattle, WA 98195, USA.

[4]National Center for Electron Microscopy, Molecular Foundry, Lawrence Berkeley National Laboratory, Berkeley, CA 94720, USA.

[5]NASA Ames Research Center, Moffett Field, CA 94035, USA.

[6]Laboratory for Space Sciences, Washington University, St. Louis, MO 63130, USA.

*Correspondence to: hope.ishii@hawaii.edu

Classification

Major: Physical Sciences

Minor: Earth, Atmospheric, and Planetary Sciences

Submitted to *Proceedings of the National Academy of Sciences*

Abstract: The solar system formed from interstellar dust and gas in a molecular cloud. Astronomical observations show that typical interstellar dust consists of amorphous (*a*-) silicate and organic carbon. *Bona fide* physical samples for laboratory studies would yield unprecedented insight about solar system formation, but they were largely destroyed. The most likely repositories of surviving presolar dust are the least altered extraterrestrial materials, interplanetary dust particles (IDPs) with probable cometary origins. Cometary IDPs contain abundant submicron *a*-silicate grains called GEMS, believed to be carbon-free. Some have detectable isotopically anomalous *a*-silicate components from other stars, proving they are preserved dust inherited from the interstellar medium. However, it is debated whether the majority of GEMS predate the solar system or formed in the solar nebula by condensation of high-temperature (>1300K) gas. Here, we map IDP compositions with single nanometer-scale resolution and find that GEMS contain organic carbon. Mapping reveals two generations of grain aggregation, the key process in growth from dust grains to planetesimals, mediated by carbon. GEMS grains, some with *a*-silicate subgrains mantled by organic carbon, comprise the earliest generation of aggregates. These aggregates (and other grains) are encapsulated in lower density organic carbon matrix, indicating a second generation of aggregation. Since this organic carbon thermally decomposes above ~450K, GEMS cannot have accreted in the hot solar nebula and formed, instead, in the cold presolar molecular cloud and/or outer protoplanetary disk. We suggest that GEMS are consistent with surviving interstellar dust, condensed *in situ*, and cycled through multiple molecular clouds.

Significance Statement: The initial solids from which the solar system formed consisted almost entirely of amorphous silicate, carbon and ices. This dust was mostly destroyed and reworked by processes that led to the formation of planets. Surviving samples of presolar dust are most likely to be preserved in comets, small cold bodies that formed in the outer solar nebula. In interplanetary dust particles originating from comets, we observe organic carbon mantles on subgrains within amorphous-silicate-dominated grains called GEMS. Our observations constrain GEMS grain formation to cold and radiation-rich environments, making a compelling case that these exotic grains, unique to a relatively obscure class of extraterrestrial material, are surviving dust from (variable) interstellar environments and thus the original building materials of planetary systems.

\body **Introduction:** Knowledge of the dust from which our molecular cloud and, later, the solar system formed is critical to our understanding of chemical and physical processes in star-forming regions, the inventory of organics incorporated in the solar system, as well as the accretion and subsequent evolution and processing of solar system bodies. Limited insight about the initial dust population has come from laboratory studies of primitive extraterrestrial objects: Some dust grains inherited from the interstellar medium (ISM) are recognizable by their dramatically non-solar isotopic compositions, and they have survived at the few to several hundred parts-per-million level in samples of primitive extraterrestrial objects. These rare, preserved "stardust grains" are the most refractory dust that formed in circumstellar outflows of other stars or supernovae and retained their isotopic signatures despite residence in the interstellar medium and solar system. However, they are a minor and unrepresentative fraction of the dust observed and modeled by astronomers (1). Most of the mass of interstellar dust (97-99%) is completely reprocessed in the interstellar medium and is subjected to shocks, impacts, recondensation and repeated cycling in and out of dense molecular clouds (2). Typical reprocessed interstellar dust grains should have averaged elemental and isotopic compositions that are similar to the sun for dust-forming elements. Although laboratory analytical studies of isotopically anomalous presolar dust have provided key insights into circumstellar environments, they cannot confidently identify most presolar dust because isotopic composition analyses in such small samples do not reliably discriminate between dust formed in the solar nebula and dust formed or accreted in the ISM.

Thus, we rely on astronomical observations and experiments to infer the characteristics of average interstellar dust that was incorporated in the solar system (1,3-6). Astronomical observations indicate that the interstellar dust incorporated in molecular clouds and cold outer nebula environments is comprised predominantly of two kinds of solids, amorphous (*a*-) silicate and organic carbon (5) (SI Appendix). Grain sizes of interstellar dust are typically 5 – 500 nm in diameter, and the *a*-silicates are inferred to be Mg-rich, likely with nanometer-scale metallic iron (5-8). Additional data was recently provided by *in situ* analysis of an ISM dust stream currently entering the solar system: The Cosmic Dust Analyzer (CDA) on board the Cassini spacecraft determined that contemporary interstellar dust grains from the diffuse ISM consist primarily of grains of magnesium-rich silicate composition with ~solar relative abundances of the non-volatile rock-forming elements Mg, Si, Ca and Fe, a mean size of ~200 nm and inferred presence

of iron inclusions (9). (Carbon detection by the CDA was difficult in such small samples impacting at high speeds due, in part, to contamination issues (9).)

The logical repositories of surviving presolar dust are small solar system bodies that escaped the differentiation processes experienced by large planetary bodies. Although rare *a*-silicate and organic carbon grains with isotopic signatures of presolar origins are found in the most primitive meteorites, the hot conditions in the inner solar nebula were not conducive to their survival (7,10). Even if such grains survived the heating, evaporation and re-condensation processes at work in the hot inner part of the solar system to be incorporated into asteroid parent bodies of meteorites, the evidence would have been largely overwritten by compaction, collisional shock, additional heating and aqueous alteration (1,11). Instead, minimally-altered primary *a*-silicates and organic carbon are most likely to survive in carbon-rich, anhydrous, interplanetary dust particles (IDPs) and micrometeorites, uncompacted dust grain aggregates believed to originate from small bodies like comets that have escaped significant alteration because of their small sizes and accretion in cold outer regions of the protoplanetary disk (12,13).

Cometary IDPs contain varying abundances of *a*-silicate grains known as GEMS (glass with embedded metal and sulfides). They are prime candidates for the initial bricks and mortar used to make planets because 1) some have been shown to have non-solar isotope compositions consistent with origins in the outflows of other stars or supernovae (14,15) and are thus unambiguous remnant interstellar dust, and 2) they have many properties consistent with those observed and inferred for interstellar dust: GEMS grains have ~solar relative abundances of the rock-forming elements, a mean grain size of ~180 nm and are unique among known meteoritic materials in having nanometer-sized inclusions of FeNi alloy (kamacite) and iron-rich sulfide (pyrrhotite) embedded in magnesium-rich, amorphous silicate glass (8,13,16-18). In addition, regions containing only GEMS grains and only organic carbon in cometary IDPs have both been shown to exhibit an ultraviolet (UV) – visible spectral feature at 5.7 eV that corresponds to the 2175 Ångstrom feature observed in the ISM and is attributed to the presence of polyaromatic hydrocarbons (PAHs) (19). Infrared spectral similarity between the organic carbon in meteorites, IDPs and dust in the (diffuse) interstellar medium has long been recognized (20). Crystalline minerals, generally believed to have been transported from hot regions of the disk, and GEMS

grains are often bound together by a typically-porous, organic carbon matrix. Organic carbon nanoglobules originating in the presolar molecular cloud or outer reaches of the protosolar disk have been reported in some cometary IDPs (21).

Two very different mechanisms and environments of GEMS formation have been proposed. The first theory proposes that GEMS formed by irradiation processing that resulted in gradual isotopic and chemical homogenization of mineral grains in a cold environment like the ISM (17). This theory posits that all GEMS are surviving presolar *a*-silicates, and only some retain detectable remnant isotope signatures of their stellar origins. The second theory proposes that most GEMS formed by non-equilibrium condensation in a hot environment like the inner solar nebula after more refractory minerals condensed from a gas of solar (elemental and isotopic) composition (18). This second theory posits that there are two populations of GEMS, some, presolar *a*-silicates, but most, solar system condensates. More details of the two theories and counterarguments are given in the SI Appendix.

Both theories for GEMS formation assume that GEMS are composed exclusively of inorganic *a*-silicate matrix and mineral grains (FeNi metal and FeNi sulfides), that is, that they are carbon-free. However, the carbon content of GEMS grains has remained elusive due to their sub-picogram masses, compositional and structural heterogeneity, terrestrial contamination, and the impracticality of gathering together such small, embedded objects to permit bulk analyses. If GEMS grains, even those that are isotopically normal, contain organic carbon, it would represent a new observational constraint on their formation conditions. Here, we describe state-of-the-art 1-3 nanometer spatial resolution analyses of GEMS to assess the petrographic (spatial) relationships between *a*-silicate and organic carbon components and consider constraints on the processes involved in GEMS formation and the astrophysical setting in which those processes most likely occurred.

Results: We examined two cometary IDPs that are rich in *a*-silicate GEMS grains and organic carbon and poor in crystalline silicates condensed in hot inner solar system regions. One contains nanoglobules. We examined a ~10 μm diameter IDP (U217B19) and a ~10 μm diameter fragment or "clast" (LT39) of a giant cluster particle (U220GCA) using electron microscopy,

149 secondary ion mass spectroscopy (SIMS) and Fourier transform infrared spectroscopy (FTIR) on
150 ultramicrotomed sections. (See SI Appendix and Fig. S1.) Both IDPs are a ~50/50% mixture by
151 volume of organic carbon and *a*-silicate GEMS (Fig. 1). The GEMS grains contain FeNi metal
152 (kamacite) and FeNi sulfide (pyrrhotite) nanocrystals embedded in amorphous Mg-silicate
153 matrix.
154
155 Energy-dispersive X-ray spectroscopy (EDX) and mapping were used to assess composition and
156 structural relationships between GEMS grains and organic carbon. Elemental mapping with 1-3
157 nm spatial resolution reveals carbon mantles both on the exterior surfaces of GEMS grains and
158 also on subgrains inside GEMS grains as well as partial mantles of GEMS material on
159 nanoglobule surfaces (Fig. 1 and SI Appendix, Table S1). Partial mantles of GEMS are identified
160 by their GEMS-like morphology and elemental chemistry. While some GEMS grains display
161 clear carbonaceous mantles on subgrains, the carbon in others is more diffusely distributed. The
162 average composition of the organic carbon matrix for U217B18, determined by STEM EDX, is
163 $C_{83}N_8O_9$ (SI Appendix, Fig. S5 and Table S2). Additional details of EDX data and procedures
164 employed are described in the SI Appendix.
165
166 Electron energy loss spectroscopy (EELS) confirms the N/C ratio of 0.07 (SI Appendix, Fig. S6
167 and Table S2). This N/C ratio is similar to that found in chondritic (CI) meteorites, although C
168 and N bulk abundances in U217B19 (and LT39) are approximately an order of magnitude
169 higher. LT39 matrix organic carbon, however, has a consistently lower N/C ratio of 0.02. From
170 relative X-ray and EELS scattering intensities, we distinguish two densities of organic carbon.
171 One is a low-density matrix, in which the GEMS grains and few crystals are embedded, and is
172 compositionally similar in both U217B19 and LT39. The other is higher density organic carbon
173 present as mantles on GEMS grains and their internal subgrains and as individual blebs in matrix
174 organic carbon (Fig. 1). Organic nanoglobules, when present, are also higher in density than the
175 surrounding matrix. The nanoglobules have O/C ratios similar to the lower density organic
176 carbon matrix, but the blebs and mantles on grains have higher O/C ratios (SI Appendix, Table
177 S2).
178
179 FTIR spectra (diffraction-limited) over entire individual thin sections show that the carbon in

U217B19 is organic. While the peak wavenumbers of several of the proposed features are not uniquely identifiable and the relative strengths of the features do not directly scale with abundances, we find that the organic carbon contains a significant aliphatic component and complex hydroxyl (R-OH), carbonyl (C=O), cyano (C≡N) and probable minor nitro ($R\text{-}NO_2$) molecular chemistry (Fig. 2). The sharp silicate feature at ~1100 cm-1 (~9 μm) is due not to GEMS but to the presence of minor crystalline silicates (pyroxene) in the ultramicrotomed section. Infrared signal from the GEMS is very weak relative to the crystalline component and is further weakened due to their high content of metal, sulfides and carbon (19). In the presence of crystalline silicates, GEMS are undetected in infrared spectra from IDP thin sections (22,23). Additional details of FTIR data and procedures employed are described in the SI Appendix.

EELS was used to investigate molecular functionality and variation at the 5 nm spatial scale in matrix organic carbon and nanoglobules (Fig. 3). Limited signal-to-noise unfortunately precluded reliable EELS collection from thin organic carbon mantles. We note, however, that the carbon within GEMS is consistent with organic matter since GEMS have a 2175 Ångstrom feature associated with PAHs in low loss EELS (24), and we see no evidence for inorganic nitride or carbide. Consistent with the FTIR data, low-loss valence-band EELS measurements from the low- and high-density organic carbon exhibit features with fine structures indicative of aliphatic and polyaromatic hydrocarbons (PAHs) and core-loss N, C and O EELS analyses indicate diverse heteroatomic N and O moieties consistent with the EDX measurements (Fig. 3b-d) (20-21,24-26). Similar hydrocarbon fine structures are observed at larger spatial scales (30-50 nm) among other IDPs and micrometeorites using synchrotron XANES (27). The EELS data reveal that molecular complexity persists to the single nanometer scale in IDPs (Fig. 3a). Additional details of EELS data and procedures employed are described in the SI Appendix.

The N, C and O isotopic compositions of IDP U217B19 were measured by ion imaging of several ultramicrotomed slices using NanoSIMS. Enrichments in ^{15}N, up to $\delta^{15}N = 412 \pm 37$ (1σ) ‰, were measured in the higher density nanoglobules in two thin sections (Fig. 4). N-rich regions elsewhere in the section correlate with locations of GEMS grains and high density organic carbon, but are not isotopically anomalous at statistically significant levels due to insufficient signal-to-noise. No statistically significant isotopic anomalies were identified in

either C or O (SI Appendix, Fig. S2). Continuous N and C signals during NanoSIMS secondary ion sputtering and imaging are consistent with organic carbon distributed throughout the volumes of GEMS grains. Additional details of NanoSIMS data and procedures employed are described in the SI Appendix.

Discussion: We report the first observation within individual GEMS grains of organic carbon mantles on *a*-silicate subgrains as small as ~10 nanometers, in addition to distinct mantles on GEMS grain exteriors (Fig. 1a-d). These GEMS and other crystalline components are bound together by an organic matrix. The organic mantles have measurably higher O contents and densities than the surrounding organic matrix. We interpret these observations as evidence for two sequential generations of aggregation, possibly in different environments. GEMS are thus first-generation aggregates in which subgrain mantles may have played a role in the aggregation (or accretion) process. The second generation of aggregation involved sticking of GEMS grains, crystals and nanoglobules, also perhaps facilitated by a second generation of mantles, to form the aggregate structure with organic matrix observed in cometary IDPs.

Organic carbon within GEMS grains clarifies our understanding of previous observations. Acid etching experiments demonstrated a close association of GEMS grains with organics that is now revealed to be even more intimate. (See SI Appendix and references therein.) Prior studies have also noted GEMS grains' anomalously low density relative to crystalline silicates, now readily explained by organic carbon within GEMS grains. Finally, observed stoichiometric excesses of oxygen were attributed solely to the *a*-silicate, but oxygen in the organic carbon also contributes to an apparent excess.

Our observations present new constraints on GEMS grains formation environment(s). The organic carbon found in GEMS interiors is inconsistent with subgrain aggregation in the hot inner solar nebula because C=O and C≡N containing molecules, like those we observe, are thermally unstable at temperatures as low as 450K (10,28). One possibility is that GEMS subgrains were transported outward from the hot inner regions, as were the minor quantities of crystalline single-mineral grains (e.g. enstatite, forsterite and pyrrhotite) that are consistent with vapor-phase condensation in the hot inner solar nebula and transport to the cold outer nebula

comet-forming region. In this case, outward-transported GEMS subgrains would have aggregated into GEMS grains in cold regions prior to the second aggregation to form cometary parent bodies. However, GEMS subgrains were not subject to the same environment as the mineral grains because the latter lack higher density mantles. This suggests that GEMS subgrains were not condensed in the inner solar system and transported outwards prior to aggregation in a colder environment. Whether or not GEMS subgrains condensed in the inner solar nebula, the presence of interior organic carbon precludes (aggregate) GEMS grain formation by non-equilibrium condensation in the inner solar system, one of the theories currently espoused for GEMS grain formation (18). It is also inconsistent with a single process in the ISM, like irradiation processing of mineral grains, the other theory for GEMS grain formation (17).

A number of lines of evidence point to cold environments for both generations of aggregation. First, GEMS-rich IDPs contain the highest abundances of surviving isotopically anomalous refractory and non-refractory components**,** consistent with a cold environment well beyond the influence of the early Sun (14,15). Second, the elemental and isotopic compositions of the organic carbon in the IDPs analyzed here support their formation in an extremely cold environment, like those in molecular clouds and/or the outer solar nebula (21,29-31). Nitrogen-rich organic carbon is believed to result from low-temperature UV photolysis of N-rich ices and (icy) mantles on grains (4,29,31). Non-solar $^{15}N/^{14}N$ isotope ratios in the nanoglobules are believed to result from chemical fractionation at even lower temperatures (~20K) (20). Different N/C element ratios in the matrix carbon of the two IDPs suggest either variability in the volatile chemistry of the molecules condensed into icy mantles prior to second generation aggregation or, more likely, differences in the temperatures and/or irradiation experienced by second generation aggregates resulting in different degrees of loss of some N-bearing species. Higher O/C ratios in the mantles on GEMS grains, relative to that in the organic matrix, are consistent with prolonged irradiation of O-bearing ices at low temperatures (20). High levels of O in organics have been previously associated with presolar molecular cloud material in IDPs (32). Third, our observations indicate that GEMS subgrains aggregated in the presence of organic nanoglobules. The organic nanoglobules in U2-17B19 exhibit inorganic, partial mantles of GEMS material on their surfaces, not previously reported (Fig. 1e-h). Nitrogen-rich, $^{15}N/^{14}N$-enriched nanoglobules have been extensively studied and require cold and radiation-rich formation environments,

273 although not necessarily simultaneously (20,21,26). As such, we infer that, like nanoglobules,
274 GEMS grains form in such environments. Finally, the mixed aliphatic and aromatic content and
275 the remarkable diversity of N- and O-bearing moieties and rich molecular heterogeneity that
276 extends down to the nanometer length scale (Figs. 2 and 3) in the organic carbon is consistent
277 with astronomical observations of rich molecular chemistry in molecular clouds (33,34).
278
279 Given the constraints on GEMS formation environments established by this study, we favor a
280 presolar origin for GEMS subgrains. Non-solar oxygen isotopic abundances detected in several
281 large GEMS grains in other IDPs show that some GEMS grains contain stardust and supernovae
282 ejecta not completely destroyed in the ISM (14,15). The observed sizes of GEMS *a*-silicate
283 subgrains are smaller than the lateral resolution in isotope measurements, suggesting that when
284 carriers of isotope anomalies are individual accreted subgrains, they may be widespread but too
285 small to be detected with current instruments. GEMS grains identified as presolar grains by
286 isotope anomalies are indisputably surviving interstellar dust. Since the vast majority (97% or
287 more) of ISM dust is expected to have formed *in situ* in dense cloud environments and, thus, be
288 isotopically ~solar*, the vast majority of GEMS grains are also consistent with dust formed *in*
289 *situ* in the ISM.
290
291 GEMS grains that contain both *a*-silicate and organic carbon have been considered in
292 astronomical observations, experiments and modeling. A core-mantle model for interstellar dust
293 was proposed decades ago but lacked confirmation in physical samples until now (36). To better
294 match astronomical observations, more recent models also incorporate physically realistic
295 composite grains having organic carbon mantles on *a*-silicate cores or aggregates of *a*-silicate
296 and organic carbon, rather than separate populations of *a*-silicate and organic carbon grains (2-
297 6). Other recent observations and models also implicate a role of organic carbon grain mantles in
298 grain aggregation (5). However, in the absence of identified physical samples, there has been
299 ongoing debate among astronomers about the significance of composite grains, either as
300 aggregates or as organic mantles on silicate grains (37,38). Specific mechanisms and
301 environments for accretion are also far from settled. Our finding of organic carbon mantles on

* With few exceptions, galactic cosmic ray measurements indicate that the interstellar dust from which they are generated is, on average, isotopically ~solar (35).

subgrains in GEMS indicates that organics or, more likely, their icy precursors were present during initial grain sticking to form first generation aggregates. Prior low resolution analyses have noted organics coating IDP components on size scales consistent with matrix organics that suggest organics or precursors were also present in the second generation of aggregation in the solar nebula (39). Some experiments and modeling find that icy, volatile-rich mantles on grains may act to facilitate grain sticking and growth of aggregates (4,40). Finally, organic mantles have been proposed to form by UV and cosmic ray irradiation of volatile ices condensed on the surfaces of exposed refractory silicate cores (4,30,31,41). We suggest that our observations can better inform future modeling.

To accommodate our observations, we propose a new GEMS formation scenario. We propose that interstellar dust experienced grain shattering (fragmentation), amorphization and sputtering erosion by supernovae shocks in the diffuse ISM as well as grain growth (recondensation) by sticking of gas-phase species to form amorphous grains of comminuted material (2,42-45). *In-situ* formation mechanisms likely account for the overwhelming majority of interstellar *a*-silicate dust (1-2,42,45,46). Additional cold condensation of refractory elements likely occurred along with volatile condensation in dense molecular clouds (2,47), where nanoglobules formed, volatile sulfur condensed, and organic-precursor-rich icy mantles grew on grain surfaces. Sticking of grains (coagulation) to form proto-aggregates may have occurred if cloud lifetimes were sufficiently long (48). With repeated cycling in and out of cold molecular clouds, mantled dust and any aggregates were repeatedly and progressively partially-destroyed and reformed. Cassini mission data suggest the presence of iron metal in contemporary interstellar dust (9). From this and nanoparticulate metal observed in ion-irradiated silicates, we infer that irradiation in the diffuse ISM (by cosmic rays, for example) likely deposited sufficient energy to permit aggregation within the amorphous silicates of handfuls of metal atoms into nanometer-sized grains of FeNi metal. Upon collapse of the presolar molecular cloud and protoplanetary disk formation, the first generation aggregate GEMS and nanoglobules, inherited from cycles through many prior molecular cloud environments and the presolar molecular cloud, were brought together with crystalline grains, likely transported from hot regions of the inner solar nebula, for the second generation of aggregation to form aggregate particles like IDPs that were incorporated in small, icy, cometary bodies. We suggest the second aggregation occurred in the

outer regions of the collapsing cloud or young protoplanetary disk subsequent to silicate condensation at high temperatures. The high abundance of GEMS grains in some cometary IDPs (~100% of nominally-inorganic grains in some cases) indicates that the outermost regions were dominated by *a*-silicate-rich grains. To produce the observed N-bearing complex organics in the organic matrix, ice-mantled grains must have experienced a radiation-rich environment prior to their incorporation in a larger parent body. Vertical diffusion of dust above the midplane of the protoplanetary disk to warmer layers, even at large heliocentric distances, may have served this role (31). Thus, nanoglobules, GEMS grains, and their high-density mantles are all consistent with products of repeated cycling in and out of cold molecular clouds followed by radiation exposure outside of, or in, optically thin regions near the edge of the solar accretion disk formed from our presolar molecular cloud.

This proposed scenario addresses additional observations about GEMS. All GEMS grains, including those that are isotopically anomalous, show nanometer-scale elemental composition heterogeneity (17,18), and it is often only collectively that GEMS grains are ~solar in elemental composition. Elemental heterogeneity is expected if the population of initial, nanometer-scale grains, from which GEMS grains subsequently aggregated, were comprised of ISM-condensed grains and partially-destroyed stellar grain fragments that acted as substrates for ISM-condensation, physically separated by icy/organic mantles. We note that other researchers have proposed near-solar elemental compositions (e.g. ±20%) as a means of identifying interstellar dust that does not display detectable isotopic anomalies (18,49); however, incomplete ISM processing of the sub-components in a dust grain, combined with chemical affinities, may produce objects that retain sufficient elemental compositional heterogeneity to be non-solar but without sufficient isotopic compositional heterogeneity to be detectable by lower spatial resolution isotope analyses.

Conclusion: This analytical study provides new constraints on the formation conditions and aggregation processes resulting in GEMS grains in cometary IDPs by demonstrating that they are comprised of organic-mantled, *a*-silicate subgrains. These observations restrict GEMS formation by aggregation to cold environments and strengthen links to presolar interstellar dust. We favor a scenario involving cycling between dense molecular cloud and diffuse ISM environments to

form *a*-silicate subgrains and suggest that GEMS aggregates may have formed in the presolar molecular cloud. Then, final aggregation of GEMS together with other IDP components may have occurred in the collapsing cloud or outer regions of the proto-planetary disk. In this scenario, GEMS acted as the original bricks and mortar of the solar system, carrying rock-forming elements and organic carbon with diverse molecular chemistry from the cold ISM into the solar nebula where remnants are preserved in small icy bodies that have avoided significant thermal and aqueous processing. There is more work to be done to fully illuminate the earliest stages of solar system body formation, and the results of this study may serve to motivate additional analyses, observations and modeling.

Acknowledgments: We dedicate this work in memory of Christine Floss, our friend and colleague, whose passion, talent, dedication, care and thoughtfulness are sorely missed. We thank E. Dobrica, F. Ciesla, G. Flynn, D. Glavin, S. Sandford, S. Wirick, A. Westphal and H. Yubata for useful discussions. We also thank the anonymous reviewers of this manuscript and of an earlier version of this manuscript. Portions of this work were performed at the Molecular Foundry and the Advanced Light Source at Lawrence Berkeley National Laboratory, which are supported by the Office of Science, Basic Energy Sciences, U.S. Department of Energy under Contract No. DE-AC02-05CH11231. HAI acknowledges funding by NASA's Laboratory Analysis of Returned Samples and Emerging Worlds Programs (NNX14AH86G and NNX16AK41G). JPB acknowledges funding by NASA's Cosmochemistry Program (NNX14AI39G). CF acknowledges funding by NASA's Cosmochemistry Program (NNX14AG25G). Data reported in this paper are archived online in the SI Appendix and available upon request to HAI.

Methods: IDP samples were prepared by ultramicrotomy and analyzed by transmission electron microscopy using imaging to study petrography, energy dispersive x-ray spectroscopy for elemental compositions and mapping, and electron energy loss spectroscopy for organic composition and bonding analyses. Secondary ion mass spectroscopy using NanoSIMS provided C, N, and O isotopic composition mapping. Fourier transform infrared spectroscopy spectra were acquired using a synchrotron source over entire samples. The multiple methods used in this study are identified in the Results section and described in more detail in the SI Appendix.

395
396

References

1. Hoppe P, Leitner J and Kodolányi J (2017) The stardust abundance in the local interstellar cloud at the birth of the Solar System. *Nature Astron.* 1:617-620.

2. Zhukovska S, Gail H-P and Trieloff M (2008) Evolution of interstellar dust and dust in the solar neighborhood. *Astron. Astrophys.* 479:453-480.

3. Jones AP, Köhler M, Ysard N, Bocchio M. and Verstraete L (2017) The global dust modeling framework THEMIS12. Gail H-P and Hoppe P (2010) The origins of protoplanetary dust and the formation of accretion disks. *Protoplanetary Dust*, eds Apai D, Lauretta DS (Cambridge Univ. Press, New York), pp 27–65.

4. Ysard N, Köhler M, Jones A, Dartois E, Godard M and Gavilan L (2016) Mantle formation, coagulation, and the origin of cloud/core shine. II. Comparison with observations. (2016). *Astron. Astrophys.* 588:A44.

5. Jones A (2014) The physical and compositional properties of dust: what do we really know? Proceedings of Science (*The Life Cycle of Dust in the Universe: Observations, Theory, and Laboratory Experiments* - LCDU 18-22 November 2013, Taipei Taiwan) 20 pp.

6. Dwek E (2016) Iron: a key element for understanding the origin and evolution of interstellar dust. *Astrophys. J.* 825:136-142.

7. Nuth JA, Rietmeijer FJM, Hill HGM (2002) Condensation processes in astrophysical environments: The composition and structure of cometary grains. *Met. Planet. Sci.* 37:1-11.

8. Goodman AA and Whittet DCB (1995) A point in favor of the superparamagnetic grain hypothesis. *Astrophy. J.* 455:L181-L184.

9. Altobelli N et al. (2016) Flux and composition of interstellar dust at Saturn from Cassini's Cosmic Dust Analyzer. *Science* 352:312-318.

10. Fray N et al. (2004) Experimental study of the degradation of polymers: Application to the origin of extended sources in cometary atmospheres. *Met. Planet. Sci.* 39:581–587.

11. Gail H-P and Hoppe P (2010) The origins of protoplanetary dust and the formation of accretion disks. *Protoplanetary Dust*, eds Apai D, Lauretta DS (Cambridge Univ. Press, New York), pp 27–65.

12. Taylor, S. S, D. E. Brownlee and G. J. Flynn eds. (2016) Cosmic Dust. *Elements* 12:159-162.

13. Bradley JP (2014) Early solar nebula grains – interplanetary dust particles. *Treatise of Geochemistry*, 2nd ed, eds Holland H, Turekian K (Elsevier-Pergamon, Oxford) pp. 297-308.

14. Messenger S, Keller LP, Stadermann F J, Walker RM and Zinner E (2003) Samples of Stars Beyond the Solar System: Silicate Grains in Interplanetary Dust. *Science* 300:105-108.

15. Floss C et al. (2006) Identification of isotopically primitive interplanetary dust particles: A NanoSIMS isotopic imaging study. *Geochim. Cosmochim. Acta* 70:2371-2399.

16. Dobrica E, Engrand C, Leroux H, Rouzaud J-N and Duprat J. (2012) Transmission electron microscopy of CONCORDIA ultraCarbonaceous Antarctic micrometeorites (UCAMMs): Mineralogical properties. *Geochim. Cosmochim. Acta* 76:68-82.

17. Bradley JP (1994) Chemically anomalous, preaccretionally irradiated grains in interplanetary dust from comets. *Science* 265:925-929.

18. Keller LP and Messenger S (2011) On the origin of GEMS grains. *Geochim. et Cosmochim. Acta* 75:5336-5365.

19. Bradley JP et al. (1999) An infrared spectral match between GEMS and interstellar grains. *Science* 285:1716-1718.

20. Alexander CMO'D, Cody GD, De Gregorio BT, Nittler LR and Stroud RM (2017) The nature, origin and modification of insoluble organic matter in chondrites, the major source of Earth's C and N. *Chemie der Erde* 77:227-256.

21. Nakamura-Messenger K, Messenger S, Keller LP, Clemett SJ and Zolensky ME (2006) Organic globules in the Tagish Lake meteorite: Remnants of the protosolar disk. *Science* 314:1439-1442.

22. Sandford SA and Walker RM (1985) Laboratory infrared transmission spectra of individual interplanetary dust particles from 2.5 to 25 microns. *Astrophys. J.* 291:838-851.

23. Bradley JP, Humecki HJ and Germani MS (1992) Combined infrared and analytical electron microscope studies of interplanetary dust particles. *Astrophys. J.* 394:643-651.

24. Bradley JP et al. (2005) An astronomical 2175 Å feature in interplanetary dust particles. *Science* 307:244-247.

25. Keller JW, Coplan MA and Goruganthu R (1992) Electron energy loss spectra of polycyclic aromatic hydrocarbons. *Astrophys. J.* 391:872-875.

26. De Gregorio B et al. (2013) Isotopic and chemical variation of organic nanoglobules in primitive meteorites. *Met. Planet. Sci.* 28:904-928.

27. Flynn GJ, Keller LP, Feser M, Wirick S and Jacobsen C (2003) The origin of organic matter in the solar system: Evidence from interplanetary dust particles. *Geochim. Cosmochim. Acta.* 67:4791-4806.

488 28. He A and Smith MA (2014) Solubility and stability investigation of Titan aerosol analogs:
489 New insight from NMR analysis. *Icarus* 232:54-59.
490
491 29. Dartois E et al. (2013) UltraCarbonaceous Antarctic micrometeorites, probing the Solar
492 System beyond the nitrogen snow-line. *Icarus* 224:243-252.
493
494 30. Jones AP et al. (2013) The evolution of amorphous hydrocarbons in the ISM: dust modelling
495 from a new vantage point, *Astron. & Astrophys.* 558:A62.
496
497 31. Ciesla F and Sandford SA (2012) Organic synthesis via irradiation and warming of ice grains
498 in the solar nebula. *Science* 336:452-455.
499
500 32. Vollmer C et al. (2014) Fluid-induced organic synthesis in the solar nebula recorded in
501 extraterrestrial dust from meteorites. *Proc Natl Acad Sci* 111:15338-15343.
502
503 33. Dartois E et al. (2007) IRAS 08572+3915: constraining the aromatic versus aliphatic content
504 of interstellar HACs. Astron. Astrophys. 463:635-640.
505
506 34. Ehrenfreund P and Charnley SB (2000) Organic Molecules in the Interstellar Medium,
507 Comets, and Meteorites: A Voyage from Dark Clouds to the Early Earth. *Ann. Rev. Astron.*
508 *Astrophys.* 38:427-483.
509
510 35. Wiedenbeck ME (1984) The isotopic composition of cosmic rays. *Adv. Space Res.* 4:15-24.
511
512 36. Greenberg JM and Li A (1996) The Core-Mantle Interstellar Dust Model. *The Cosmic Dust*
513 *Connection,* ed Greenberg JM (Kluwer Academic Publishers, Dortrecht) pp. 43-70.
514
515 37. Jones A (2015) Interstellar dust modelling: Interfacing laboratory, theoretical and
516 observational studies (The THEMIS model). *Proc Internatl Astron Union* 11(A29A): pp 313-
517 316.
518

519 38. Li Q, Liang SL and Li A (2014) Spectropolarimetric constraints on the nature of interstellar
520 grains. *Mon. Not. R. Astr. Soc.* 440:L56-L60.
521
522 39. Flynn GJ, Wirick S and Keller LP (2013) Organic grain coatings in interplanetary dust
523 particles: Implications for grain sticking in the Solar Nebula. *Earth Planets Space* 65:1159-1166.
524
525 40. Supulver KD, Bridges FG, Tiscareno S, Lievore H and Lin DNC (1997) The sticking
526 properties of water frost produced under various ambient conditions. *Icarus* 129:539-554.
527
528 41. Kimura H, Wada K, Senshu H and Kobayashi H (2015) Cohesion of amorphous silica
529 spheres: toward a better understanding of the coagulation of silicate dust aggregates.
530
531 42. Jones AP, Tielens AGGM, Hollenbach DJ and McKee CF (1994) Grain destruction in shocks
532 in the interstellar medium. *Astrophys.* 433:797-810.
533
534 43. Draine BT (2003) Interstellar dust grains. *Ann. Rev. Astron. Astrophys.* 41:241-289.
535
536 44. Kemper F, Briend WJ and Tielens AGGM (2004) The absence of crystalline silicates in the
537 diffuse interstellar medium. *Astrophys. J.* 609:826-837.
538
539 45. Zhukovska S, Dobbs C, Jenkins EB and Klessen RS (2016) Modeling dust evolution in
540 galaxies with a multiphase, inhomogeneous ISM. *Astrophys. J.* 831:147 (15pp).
541
542 46. Mathis JS, Rumpl W and Nordsieck KH (1977) The size distribution of interstellar grains.
543 *Astrophys. J.* 217:425–433.
544
545 47. Rouillé G et al (2014) Cold condensation of dust in the ISM. *Faraday Discussions* 168:449-
546 460.
547

548 48. Ormel CW, Paszun D, Dominik C and Tielens AGGM (2009) Dust coagulation and
549 fragmentation in molecular clouds. I. How collisions between dust aggregates alter the dust size
550 distribution. *Astron. & Astrophys.* 502: 845-869.
551
552 49. Alexander CMO'D, Nittler LR, Davidson J, Ciesla FJ (2017) Measuring the level of
553 interstellar inheritance in the solar protoplanetary disk. *Met. Planet. Sci.* 52:1797-1821.

Figure Legends

Figure 1: Petrographic relationship between organic carbon and amorphous silicates in cometary IDPs. (a) High angle annular darkfield (HAADF) image of a section through the middle of a single GEMS grain in U217B19 and (b) Corresponding carbon element map showing organic rims on subgrains within the GEMS grain. (c) HAADF image of a section through the middle of a GEMS grain in LT39 and (d) corresponding carbon element map showing a higher brightness organic carbon rim mantling the GEMS exterior surface. The higher brightness rim corresponds to higher-density organic carbon with higher C/O ratio (See SI Appendix). (e) HAADF image of PAH-rich nanoglobules (ng) comprised of higher-density organic carbon and (f) element map. Red=C, blue=Mg, green=Fe and yellow=S. One nanoglobule has a partial GEMS mantle shown in inset. (g) HAADF image of a nanoglobule heavily decorated with GEMS. (h) Brightfield image of two carbon-rich GEMS, with one on right a torus with an organic carbon interior and inorganic exterior.

Figure 2: Synchrotron FTIR spectrum from a thin section of IDP U217B19 mounted on a carbon film substrate TEM grid. The spectrum allows definitive assignments of hydroxyl (-OH), aliphatic hydrocarbon (-CH_3, CH_2), carbonyl (C=O), and silicate (SiO_x) functional groups. Despite the predominance of amorphous silicate in the section volume, the silicate feature is relatively narrow due to the strong signal from the (minor) crystalline silicates that are present. The spectral features also indicate the possible presence of cyano (C≡N) and nitro groups (R-NO_2).

Figure 3: Electron energy-loss spectra from organic carbon in U217B19. **(a)** Low-loss spectra from matrix (a.1) and nanoglobule (a.2) displaying a prominent ~5.5 eV feature characteristic of polyaromatic hydrocarbons (PAHs). **(b)** Core loss carbon-K edges from two different regions of the organic matrix (b.1&b.2), a nanoglobule (b.3) and the carbon support substrate (b.4). Fine structures on the edges are consistent with the following functional groups: aliphatic and/or aromatic ring -C=C-; imine C=N; aldehydes O=CH, ketones C=O, nitrile C≡N; aliphatic C=C; amide O=C-NH_x, carboxyl O=C-O. (See SI Appendix for peak assignments.) **(c)** Nitrogen-K edge with a feature at 401.5 eV consistent with nitrile and/or amide functionalities. **(d)** Oxygen-

585 K edge with a sharp pre-edge feature at 531 eV consistent with carbonyls (C=O).
586
587 **Figure 4:** (a) Ion-induced secondary electron image of a region of thin section of U217B19 and
588 (b) corresponding $\delta^{15}N$ intensity map. The ^{15}N-rich hotspot in the rectangle corresponds to the
589 enlarged region in d) and has $\delta^{15}N = 412 \pm 37$ ‰. Black regions correspond to locations with
590 insufficient N to determine isotopic ratios, typically low density organic carbon matrix. Other N-
591 rich regions correspond to areas in which GEMS and high density organic carbon are present but
592 with insufficient signal-to-noise to determine isotopic anomalies at a statistically significant
593 level. (c) HAADF image of thin section of U217B19. Rectangle indicates the location of the
594 enlarged region in d). (d) HAADF image of the region containing the ^{15}N-rich hotspot shows that
595 it corresponds to a high density organic carbon nanoglobule (ng). The darker region labeled "c"
596 is lower density organic carbon.

Figure 1

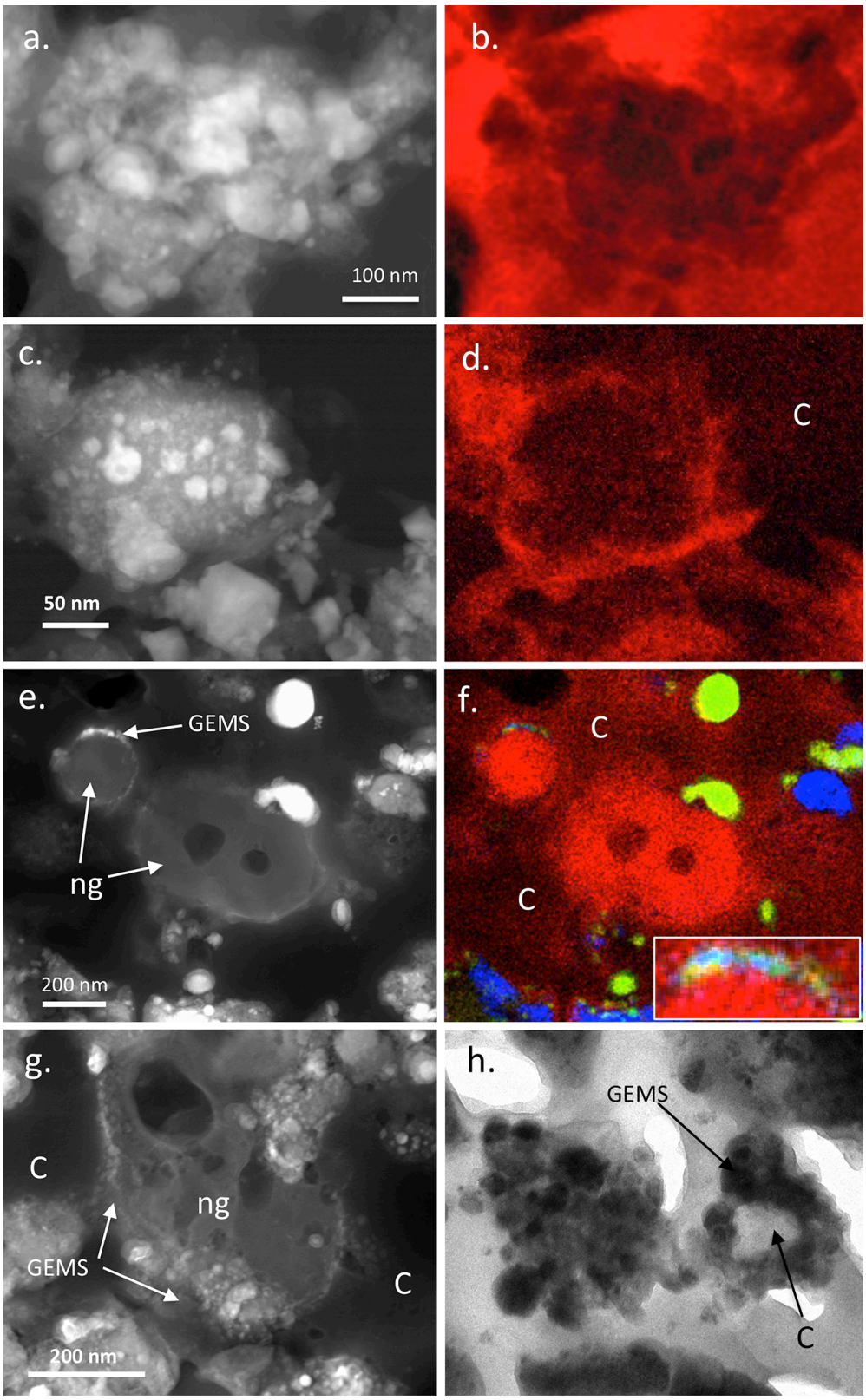

Figure 2

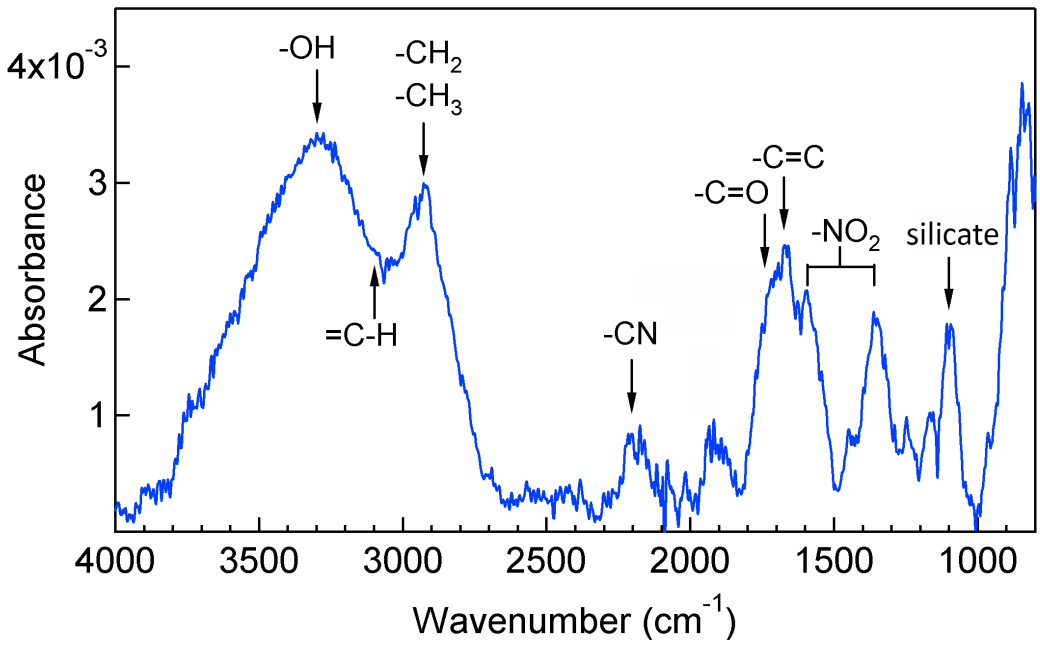
4x10-3
3
2
1
Absorbance
-OH
-CH2
-CH3
=C-H
-CN
-C=C
-C=O
-NO2
silicate
4000
3500
3000
2500
2000
1500
1000
Wavenumber (cm-1)

Figure 3

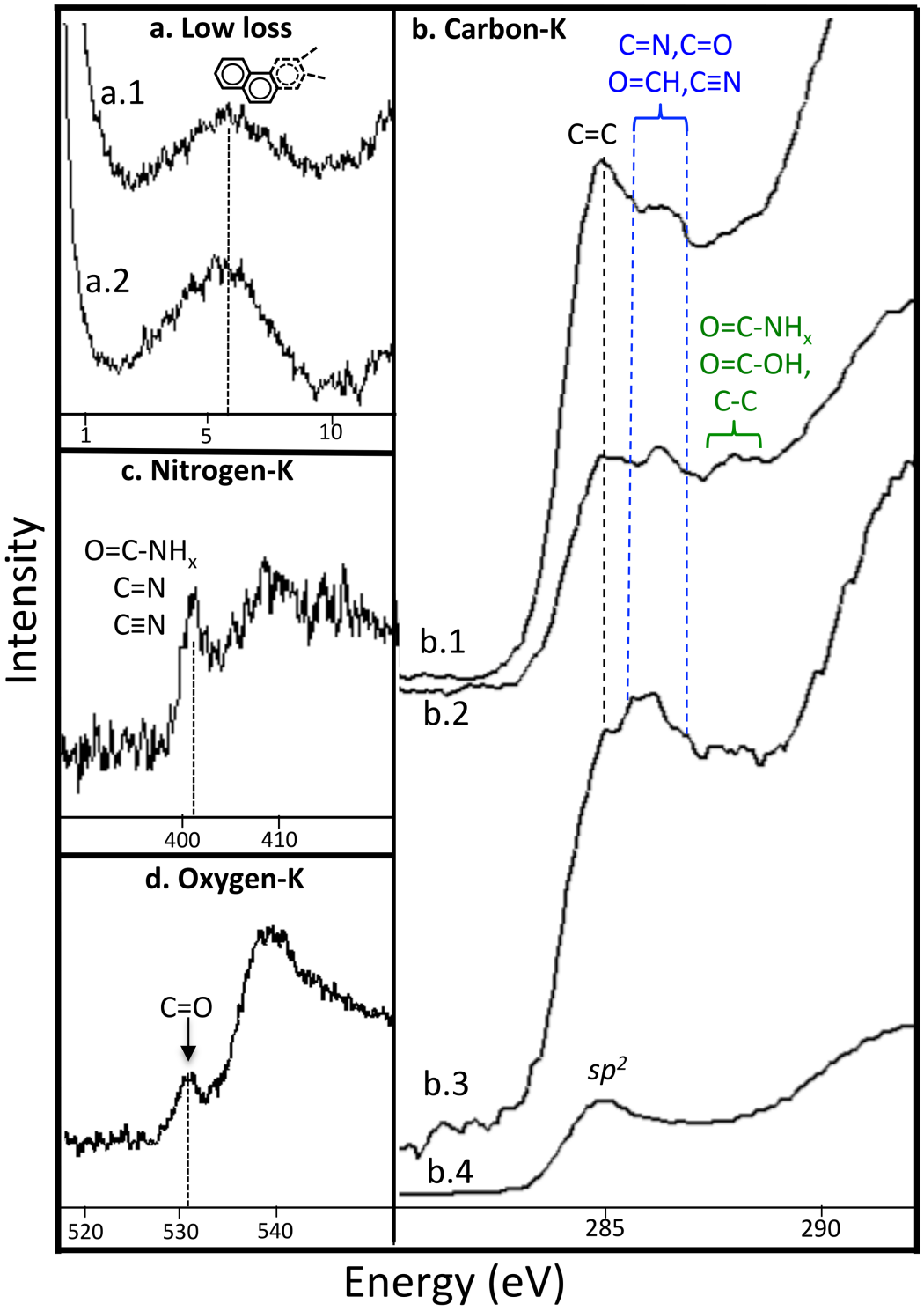
a. Low loss
a.1
a.2
1
5
10
b. Carbon-K
C=N,C=O
O=CH,C≡N
C=C
O=C-NHx
O=C-OH,
C-C
b.1
b.2
b.3
b.4
sp2
285
290
c. Nitrogen-K
O=C-NHx
C=N
C≡N
400
410
d. Oxygen-K
C=O
520
530
540
Intensity
Energy (eV)

Figure 4